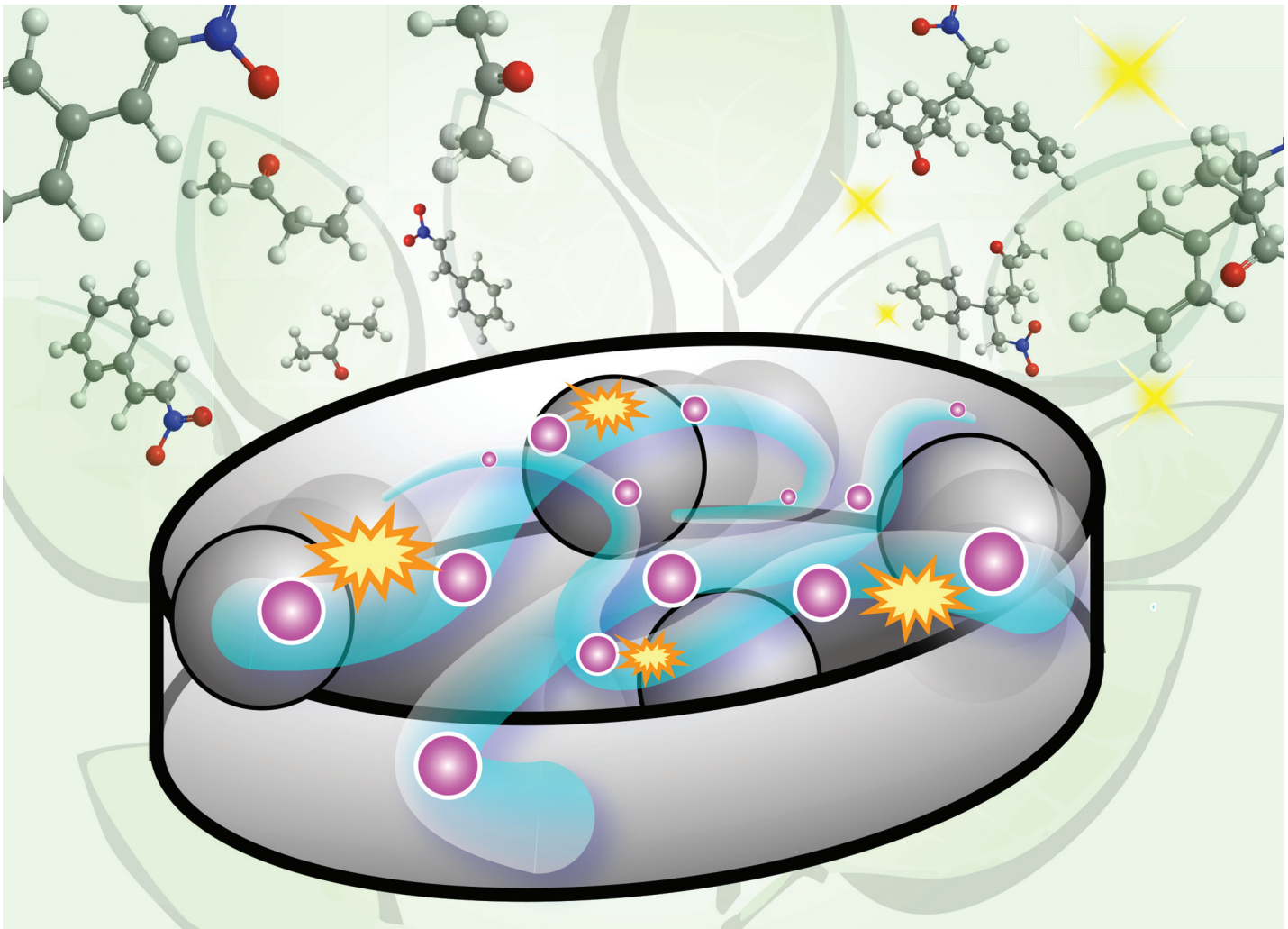

Showcasing research from Professor Miura's laboratory, School of Chemical Engineering, University of Kyushu, Fukuoka, Japan.

Solvent-less mechanochemical asymmetric reactions in a ball mill utilizing a polymer-supported Hayashi–Jørgensen catalyst: effects of the polymer backbone and flexibility on its catalytic performance

A polymer-supported organocatalyst was developed for solvent-less mechanochemical synthesis. The polymer functioned as a grinding additive for dispersion of solid substrates and stabilization of the supported organocatalyst. A correlation was observed between the polymer's glass transition temperature and the catalytic performance, where the polymer flexibility was a key for superior catalytic performance. This catalyst design provides a sustainable and eco-friendly pathway for high-value fine chemical production, advancing the goals of green chemistry.

Image reproduced by permission of Hikaru Matsumoto from *Green Chem.*, 2026, **28**, 3141.

As featured in:

See Hikaru Matsumoto, Yoshiko Miura *et al.*, *Green Chem.*, 2026, **28**, 3141.

ROYAL SOCIETY OF CHEMISTRY

rsc.li/greenchem

Registered charity number: 207890

Green Chemistry

PAPER

View Article Online
View Journal | View Issue

Check for updates

Cite this: *Green Chem.*, 2026, **28**, 3141

Solvent-less mechanochemical asymmetric reactions in a ball mill utilizing a polymer-supported Hayashi–Jørgensen catalyst: effects of the polymer backbone and flexibility on its catalytic performance

Kento Hiroishi,[a] Hikaru Matsumoto, *[a] Hidetaka Kasai, [b] Masanori Nagao, [a] Eiji Nishibori [c] and Yoshiko Miura *[a]

Received 7th October 2025,
Accepted 22nd December 2025

DOI: 10.1039/d5gc05291b

rsc.li/greenchem

Fine chemical synthesis under solvent-free or solvent-less mechanochemical conditions is highly desirable from a green chemistry perspective. However, the inherently low contact efficiency between the catalyst and solid substrates often results in low reaction efficiency. Polymer-assisted grinding (POLAG) in a ball mill has been developed for solvent-less organic synthesis, where polymers are used as additives to effectively disperse solid reactants. Specifically, polymer-supported catalysts have been shown to function as POLAG additives to enhance catalytic performance. However, the effects of the structures of polymer-supported catalysts on their catalytic performance have not been fully investigated. Here, we prepared polymer-supported catalysts bearing the Hayashi–Jørgensen catalyst with different polymer backbones and chemical structures of spacer monomers. In an asymmetric Michael addition reaction in the presence of solid reactants in a ball mill, the polymer-supported catalyst exhibited a significantly higher turnover number compared to its small-molecule counterpart. Additionally, a correlation between the glass transition temperature of the polymer-supported catalyst and the turnover frequency was confirmed, which suggested that the flexible polymer support facilitated solid dispersion and boosted subsequent catalytic cycles.

Green foundation

1. This work introduces a mechanochemistry-directed design of polymer-supported organocatalysts for solvent-less organic synthesis, which demonstrates a green and sustainable practice for producing chiral compounds *via* solvent reduction and improvement of catalytic performance.
2. The methodology can avoid bulk solvents, shorten reaction time, and prolong catalytic durability for the mechanochemical organic synthesis of fine chemicals with a ball mill. Compared with small-molecule catalysts, our polymer-supported catalyst can dramatically accelerate the catalytic reaction with a durable catalytic lifetime. Furthermore, the *E*-factor of the polymer catalyst system was much lower (0.1) than that of the solution-based system (57), aligning with green chemistry principles by solvent usage reduction and catalyst lifetime improvement.
3. Further greening can include the development of fully solvent-free asymmetric reactions and extension of this strategy to continuous-flow mechanochemistry with twin-screw extrusion, enhancing scalability and sustainability.

Introduction

Recently, sustainable development goals (SDGs) have attracted global attention. This focus has been extended to chemical production, where green chemistry is strongly related to the SDGs for environmentally benign synthetic processes.[1] Among the 12 principles of green chemistry, waste prevention is paramount. On the other hand, the present fine chemical synthesis generates a large amount of waste, such as byproducts and solvents, due to its complicated synthetic routes and low productivity and selectivity. In particular, solvent waste accounts for approximately 90% of the reagents used in fine chemical

[a]*Department of Chemical Engineering, Faculty of Engineering, Kyushu University, 744 Motooka, Nishi-ku, Fukuoka 819-0395, Japan.*
E-mail: hmatsumoto@chem-eng.kyushu-u.ac.jp, miuray@chem-eng.kyushu-u.ac.jp
[b]*Department of Materials Science, Osaka Metropolitan University, 1-1 Gakuen-cho, Naka-ku, Sakai, Osaka 599-8531, Japan*
[c]*Department of Physics, Institute of Pure and Applied Sciences and Tsukuba Research Center for Energy Materials Science, University of Tsukuba, Tsukuba 305-8571, Japan*

Open Access Article. Published on 23 December 2025. Downloaded on 6/4/2026 10:27:18 PM.
This article is licensed under a Creative Commons Attribution-NonCommercial 3.0 Unported Licence.

Open Access Article. Published on 23 December 2025. Downloaded on 6/4/2026 10:27:18 PM.
This article is licensed under a Creative Commons Attribution-NonCommercial 3.0 Unported Licence.

production.[2,3] As a key metric in green chemistry, the *E*-factor can reach up to 10^2 kg waste per kg product in the fine chemical synthesis, which is rather higher than that in bulk chemical synthesis (1–5 kg waste per kg product).[4] Thus, reduction of solvent usage in fine chemical production is crucial to achieve SDGs by the suppression of environmental footprints through green synthetic processes.

Mechanochemistry is a discipline that deals with physical and chemical changes induced by mechanical forces such as compression, shear, and friction in small molecules,[5–8] crystals,[9,10] and polymers.[11–13] Recent progress in mechanochemical protocols has witnessed the utilization of mechanochemistry in organic synthesis, which is termed "mechanochemical organic synthesis".[5,14] Mechanochemical organic synthesis is driven by mechanical energy input from sonication[13,15] and physical grinding.[16,17] Unlike traditional solution processes, ball milling processes have attracted considerable attention owing to their solvent-less conditions, shorter reaction times, and unique reactivity and selectivity.[16,17] In a ball mill, mechanical energy is transferred to substrates and catalysts by collision and friction at the surfaces of the balls and the inner wall of the jar during shaking or rotation (Fig. 1a). To date, numerous reports have demonstrated the advantages of solvent-less mechanochemical organic synthesis such as reduced solvent usage, accelerated reaction rates, and efficient conversion of hardly soluble reactants.[7,8]

One unique advantage of mechanochemical organic synthesis is that solid-state organic reactions can be promoted under solvent-less conditions. In this system, mixing efficiency is strongly correlated with the resultant reaction performance. This is primarily due to limited contact efficiency at substrate–

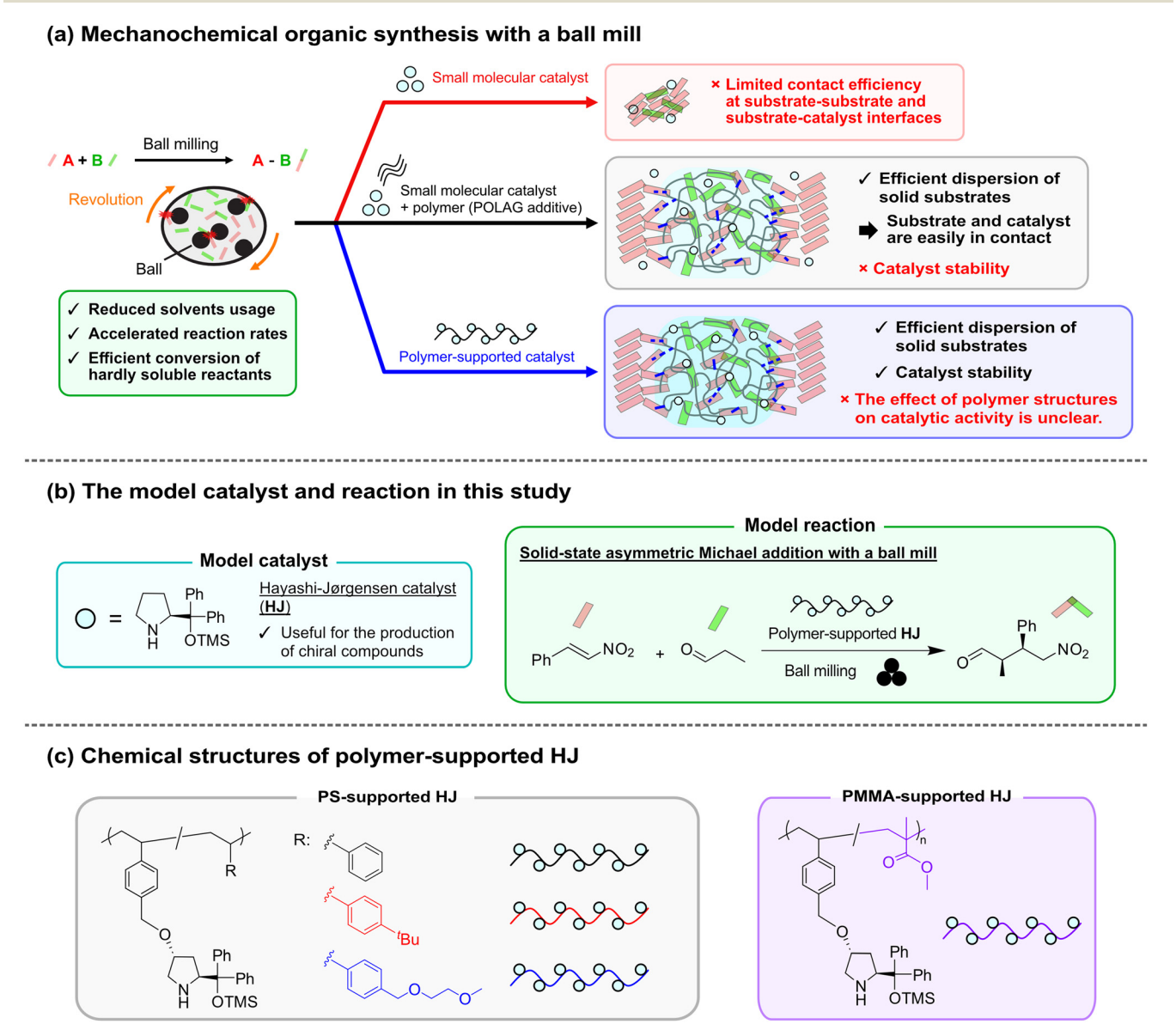

Fig. 1 (a) Mechanochemical organic synthesis with a ball mill. (b) The model catalyst (**HJ**) and reaction (solid-state asymmetric Michael addition with a ball mill) in this study. (c) Chemical structures of polymer-supported **HJ**.

This journal is © The Royal Society of Chemistry 2026

Open Access Article. Published on 23 December 2025. Downloaded on 6/4/2026 10:27:18 PM. This article is licensed under a Creative Commons Attribution-NonCommercial 3.0 Unported Licence.

substrate and substrate–catalyst interfaces in solid-state systems compared to conventional solution systems (Fig. 1a).[16] In this sense, previous studies have shown that additives could improve the mixing efficiency and the reaction yields. Liquid-assisted grinding (LAG) is one of the strategies to alter reactivity and selectivity by adding trace amounts of liquid (<2 μL liquid per mg solid).[18–20] It has been recognized that the LAG could promote partial dissolution of the solid substrate at the surfaces and increase its molecular mobility, resulting in a dramatic improvement in mixing and reaction efficiencies.[21] Another method is known as polymer-assisted grinding (POLAG), in which polymers are used as additives. For instance, Lamaty and co-workers reported the synthesis of pharmaceutical ethotoin from solid substrates using poly(ethyleneglycol) (PEG).[22,23] They also reported the application of the PEG additive to Pd-catalyzed Mizoroki–Heck reactions under solvent-free conditions.[24] Kubota and Ito reported Pd-catalyzed Suzuki–Miyaura cross-couplings in the presence of solid substrates by utilizing a poly(tetrafluoroethylene) (PTFE) additive.[25] These pioneering studies on the use of POLAG in solid-state mechanochemical organic synthesis suggest that substrate–polymer interactions at their interfaces could efficiently disperse the solid substrates and subsequently accelerate the reactions.

The merger of the POLAG strategy and excellent catalytic systems has seen significant advancement in solid-state mechanochemical organic synthesis. For example, Kubota and Ito developed phosphine–Pd catalysts covalently bound to PEG as efficient catalytic systems for solid-state Suzuki–Miyaura cross-couplings. This phosphine-PEG hybrid material featured good dispersion of solid substrates and effective suppression of Pd aggregation in the flexible PEG chains.[26] Yu and co-workers reported regioselective Heck reactions using cyclodextrin (CD)-supported Pd catalysts by leveraging the substrate inclusion properties of the CD matrix.[27] The catalyst reactivity and selectivity were significantly altered by placing the catalyst and polymer in close proximity, thereby enabling cooperative effects for efficient solid substrate dispersion, metal catalyst stabilization, and selective molecular transformations (Fig. 1a). Thus, mechanochemistry-directed catalyst design featuring unique polymer properties provides green synthetic protocols with unprecedented reactivity and selectivity. To this end, it is important to understand the polymer-supported catalyst system in solid-state mechanochemical organic synthesis. However, deep insights are still lacking. For example, the effects of polymer structure on catalytic performance have not yet been systematically investigated, which would lead to design guidelines for efficient solvent-less organic synthesis and thereby contribute to green chemistry.

Herein, we systematically elucidated the influence of polymer support structures on catalytic performance in solid-state mechanochemical synthesis. As a model catalyst, the Hayashi–Jørgensen catalyst (**HJ**) was selected, as it is a useful asymmetric organocatalyst for the synthesis of fine chemicals such as chiral γ-amino acid derivatives (Fig. 1b). The utility of **HJ** has been demonstrated not only in solution processes,[28,29] but also in mechanochemical processes using a ball mill.[30] In addition, the incorporation of the **HJ** moiety into synthetic polymers has been reported.[31–33] In this study, the polymer-supported **HJ** was synthesized through a simple radical copolymerization of vinylated **HJ** with a spacer monomer (Fig. 1b). To vary the structures of the polymer, different chemical structures of spacer monomers were copolymerized. Using the polymer catalyst, asymmetric Michael addition of aldehydes to nitroalkenes was performed under solvent-less conditions using a planetary ball mill (Fig. 1b). *In situ* powder X-ray diffraction (PXRD) analysis during ball milling was performed to monitor the solid state of the reaction mixture. Comparative experiments with small-molecule counterparts were performed to highlight the superior catalytic performance of polymer-supported **HJ**. Through the systematic investigation of the series of polymer catalysts, we found a correlation between the chemical structure of the spacer monomer and catalytic performance, which was explained by the flexibility of the polymer-supported catalyst. Furthermore, green chemistry metrics (*e.g.*, *E*-factor, process mass intensity (PMI), and solvent intensity (SI)) were estimated for the present catalytic system for the contribution of polymer-supported **HJ** to sustainable and green organic synthesis through waste prevention.

Results and discussion

Reaction condition screening for Michael addition with a ball mill

We first screened the mechanochemical conditions for the Michael addition reaction between (*E*)-β-nitrostyrene (**1a**) and propionaldehyde (**2a**). The reactants were placed in a ZrO_2 milling jar with ZrO_2 balls and milled in a planetary ball mill. After 4 h, the milling was stopped, followed by opening the jar to analyze the reaction mixture. In the absence of **HJ**, no generation of product (**3a**) from the Michael addition was observed (entry 1, Table 1). On the other hand, the addition of **HJ** achieved a significant conversion to the product (51% yield, entry 2). At different revolution rates (200 and 400 rpm), no significant difference in the yields was observed (51% and 41%, respectively, entries 2 and 3). Both conditions showed excellent diastereoselectivity, indicating a stereoselective reaction in the ball mill (94 : 6 and 87 : 13 *syn*/*anti*, respectively, entries 2 and 3). However, a black powder was observed in the reaction mixture processed at 400 rpm (Fig. S2a–c). Energy dispersive X-ray spectroscopy (EDX) analysis revealed that this powder was mainly composed of Zr (Fig. S2d). This suggested that ZrO_2 powder from the jar and balls contaminated the reaction mixture due to vigorous milling and abrasion. No abrasion of the jar or balls occurred at 200 rpm. Thermographic analysis showed that the temperature of the reaction mixture was approximately 30 °C immediately after opening the milling jar (Fig. S3). This confirmed that there was no excessive heat generation and reaction promotion under the ball milling conditions.

By fixing the revolution rate at 200 rpm and increasing the catalyst loading to 5 and 10 mol%, the yields increased to 99 and 94%, respectively (entries 4 and 5). On the other hand, a

Open Access Article. Published on 23 December 2025. Downloaded on 6/4/2026 10:27:18 PM.
This article is licensed under a Creative Commons Attribution-NonCommercial 3.0 Unported Licence.

Table 1 Screening of reaction conditions for asymmetric Michael addition reactions[a]

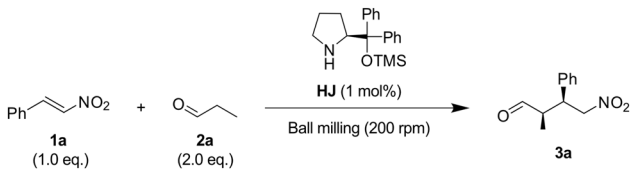

Entry	Revolution rate [rpm]	Reaction time [h]	Catalyst [mol%]	Yield[c] [%]	*syn*/*anti*[c]
1	200	4	—	Trace	n.d.
2	200	4	1	51	94 : 6
3	400	4	1	41	87 : 13
4	200	4	5	99	65 : 35
5	200	4	10	94	67 : 33
6[b]	—	24	1	38	94 : 6

[a] Reaction conditions: **1a** (1.8 mmol, 1.0 eq.), **2a** (3.6 mmol, 2.0 eq.) and **HJ** were milled in a 20 mL ZrO_2 jar with four ZrO_2 balls (Φ = 10 mm) under an ambient atmosphere. [b] Reaction conditions: **1a** (1.8 mmol, 1.0 eq.), **2a** (3.6 mmol, 2.0 eq.), and **HJ** were stirred in toluene (9 mL) at 25 °C with a magnetic stirring bar. [c] Determined by HPLC.

decrease in stereoselectivity was observed (65 : 35 and 67 : 33 *syn*/*anti*), suggesting that an increase in the contact frequency between **3a** and **HJ** induced epimerization.[32] For comparison, the Michael addition reaction was performed in a solution process with toluene as the reaction solvent. Even after 24 h, the Michael addition in toluene gave a lower yield (38%, entry 6). The optimization of the reaction conditions using a ball mill allowed for the rapid and stereoselective mechanochemical organic synthesis, which highlighted the usefulness of solvent-less molecular transformations.

In situ analysis of the reaction mixture during ball milling

To clarify the state of the reaction mixture under ball milling, *in situ* PXRD was performed (Fig. S4; for details, see the SI).[34,35] A broad peak at 2θ = 5.5° was observed due to scattering from the polycarbonate (PC) milling jar used in all *in situ* PXRD analyses (Fig. 2). A mixture of **1a** and **2a** (**1a** + **2a**) was processed with the ball mill. In the *in situ* PXRD pattern of **1a** + **2a**, diffraction peaks were observed at 2θ = 3.5 and 3.9° (blue line, Fig. 2). These peaks were consistent with those obtained from milling **1a** alone (red line, Fig. 2) and the calculated pattern of **1a** based on its crystal structure (black line).[36] Next, **HJ** was added to **1a** + **2a**, and the Michael addition reaction was performed by ball milling (**1a** + **2a** + **HJ**). After milling for 1000 s, the *in situ* PXRD pattern showed complete disappearance of diffraction peaks at 2θ = 3.5 and 3.9° (green line, Fig. 2). This clearly indicated that nitroalkene **1a** initially reacted while retaining its solid crystalline domain, and finally an amorphous reaction mixture was obtained after the Michael addition reaction in the ball mill.

Throughout the *in situ* PXRD analysis, the solid reactant (**1a**) initially existed in the present catalytic system in the ball mill. In this situation, mixing of reactants and the catalyst might be severely limited under the solvent-less conditions.

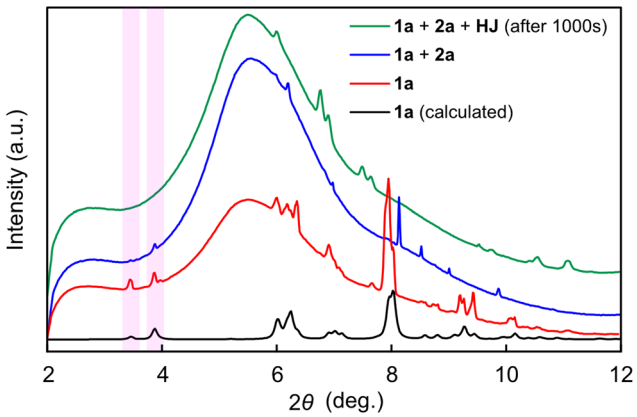

Fig. 2 *In situ* PXRD patterns of **1a**, **1a** + **2a**, and **1a** + **2a** + **HJ** during ball milling.

Using a polymer-supported catalyst as a POLAG additive, substrate–polymer interactions would efficiently disperse the solid substrates and drastically accelerate the catalytic reactions.

Synthesis of polymer-supported HJ

To further enhance the efficiency of Michael addition reactions in the presence of solids, we designed polymer-supported **HJ** that can function as POLAG additives. The polymer catalysts were synthesized by free-radical copolymerization (Fig. 3a). Styrene-type monomers containing **HJ** (**HJ monomer**) were synthesized according to the previous reports (for details, see the SI).[32,33] As spacer monomers, styrene (**S**), styrene derivatives bearing a *tert*-butyl group (**^{t}BuS**) or ethylene glycol moiety (**EGS**), or methyl methacrylate (**MMA**) were copolymerized with the **HJ monomer**. By varying the chemical structure and feed ratio of the spacer monomers, a series of polymer catalysts was prepared (**pHJ-S**, **pHJ-^{t}BuS**, **pHJ-EGS**, **pHJ-S-^{t}BuS**, **pHJ-S-EGS**, and **pHJ-MMA**) (Table S1). All polymers were obtained as white or yellowish powders (28–69% yield). ^{1}H NMR analysis confirmed the incorporation of **HJ** into the polymers ([**HJ**] = 0.39–1.29 mmol g^{-1}, Fig. S9–14). Size-exclusion chromatography (SEC) analysis confirmed unimodal molecular weight distributions (8900–38 300 g mol^{-1}, Fig. 3b and S15). DSC measurements for the polymers were performed to obtain the glass transition temperature (T_g) (Fig. 3c). T_g is a thermophysical property that correlates with polymer chain flexibility (a lower T_g indicates higher polymer chain flexibility). The T_g of the polymer catalysts with different spacer structures ranged from 22.8 to 137.1 °C, strongly depending on the chemical structure of the spacer monomer and the feed ratio. Notably, the introduction of ethylene glycol units dramatically lowered the T_g of the polymer catalysts (22.8 and 57.9 °C for **pHJ-EGS** and **pHJ-S-EGS**, respectively). This suggested that the presence of flexible ethylene glycol structures enhances polymer chain flexibility.[37]

Effects of polymer backbones on catalytic performance

The Michael addition reaction was performed in a ball mill using the synthesized polymer-supported **HJ**. **pHJ-S** and

 This journal is © The Royal Society of Chemistry 2026

Open Access Article. Published on 23 December 2025. Downloaded on 6/4/2026 10:27:18 PM.
This article is licensed under a Creative Commons Attribution-NonCommercial 3.0 Unported Licence.

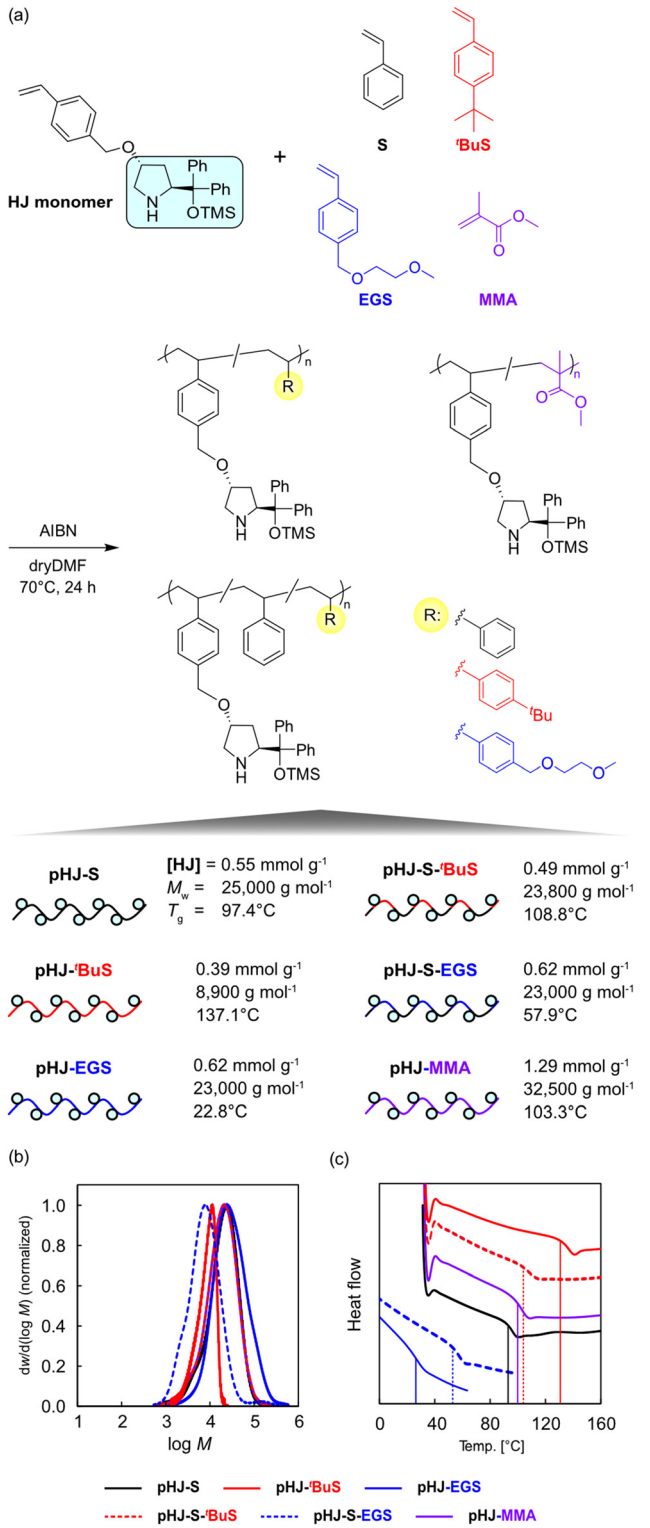

Fig. 3 (a) Synthesis of polymer-supported **HJ**. (b) SEC chromatogram of polymer-supported **HJ**. (c) DSC curves of polymer-supported **HJ** (second heating step). **pHJ-S** (solid black line), **pHJ-^{t}BuS** (solid red line), **pHJ-EGS** (solid blue line), **pHJ-S-^{t}BuS** (dashed red line), **pHJ-S-EGS** (dashed blue line), and **pHJ-MMA** (solid purple line).

pHJ-MMA, which had comparable T_g (97.4 and 103.3 °C), were first tested in the mechanochemical Michael addition reaction. The catalyst loading was fixed at 1 mol% to achieve high diastereoselectivity (Table 1). The mechanochemical reactions were performed in different batches with varying reaction times to obtain a time–yield profile (Fig. 4). All polymer catalysts showed comparable stereoselectivity with **HJ** (84 : 16–91 : 9 *syn*/*anti*, Table 2). In the initial reaction time (0.25 to 0.5 h), the yield increased almost proportionally with increasing reaction time. Interestingly, in the initial reaction time, the turnover frequencies (TOFs) of **pHJ-S** and **pHJ-MMA** (64 and 62 h^{-1}, respectively) were significantly higher than that of **HJ** (54 h^{-1}, Table 2). After 1 h, however, the reaction drastically slowed, except for the **pHJ-S** system. The turnover numbers (TONs) at a reaction time of 4 h were 51, 84, and 68 for **HJ**, **pHJ-S**, and **pHJ-MMA**, respectively. It should be noted that the TON of **pHJ-S** was 1.6-fold higher than that of **HJ**. No clear correlation was found between catalytic activity and molecular weight or catalyst loading in the **pHJ-S** system (Tables S2 and S3). When **HJ** was mixed with catalyst-free polystyrene (PS) as a POLAG additive (**HJ** + PS), **HJ** exhibited a high TOF (106 h^{-1}, Table 2), but the TON was still low (47).

As expected, the polymer backbone of the catalyst functioned as a POLAG additive by effectively dispersing solid substrates to increase the contact efficiency between the reactants and the catalyst to improve the TOF. It is noteworthy that the TON also dramatically increased by using **pHJ-S**. To gain insight into this amazingly high catalyst durability, the reaction mixture was analyzed by SEC and ^{1}H NMR spectroscopy after the catalytic reaction in the ball mill for 4 h. The SEC analysis of the spent **pHJ-S** showed that the molecular weight remained almost the same before and after the reaction (Fig. S16). On the other hand, a drastic decrease in the ^{1}H NMR peak integral of the methyl protons of the TMS group on the **HJ** unit was observed (Fig. S17). Based on the peak integral

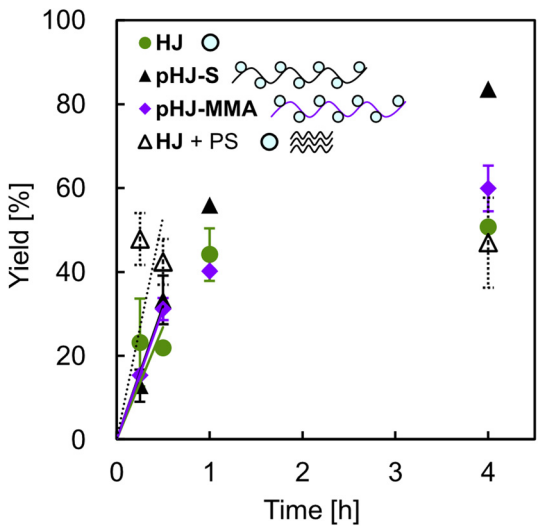

Fig. 4 Time–yield profile for solvent-less Michael addition using ball milling with **HJ**, **pHJ-S**, **pHJ-MMA**, and **HJ** + PS.

Open Access Article. Published on 23 December 2025. Downloaded on 6/4/2026 10:27:18 PM.
This article is licensed under a Creative Commons Attribution-NonCommercial 3.0 Unported Licence.

Table 2 Solvent-less Michael addition using ball milling with **HJ** and polymer-supported **HJ**[a]

Catalyst	TOF [h^{-1}][b,c]	TON [—][b]	*syn* : *anti*[b]
HJ	54	51	90 : 10–94 : 6
pHJ-MMA	62	68	88 : 12–91 : 9
pHJ-S	64	84	84 : 16–90 : 10
HJ + PS	106	47	91 : 9–95 : 5

[a] Reaction conditions: **1** (1.8 mmol, 1.0 eq.), 2 (3.6 mmol, 2.**0** eq.) and catalyst (1 mol% as **HJ** unit) were milled in a 20 mL ZrO_2 jar with four ZrO_2 balls (Φ = 10 mm) under an ambient atmosphere. [b] Determined by HPLC. [c] Determined at reaction times from 0.25 to 0.5 h.

ratio of the TMS group to the methylene protons on the five-membered ring of the **HJ** unit, it was confirmed that only 20% and 22% of the TMS groups remained in the spent **HJ** and **pHJ-MMA**, respectively. Surprisingly, 49% of the TMS groups remained in the spent **pHJ-S**.

From the ^{1}H NMR analyses, degradation of the TMS group in **HJ** was suggested, while **pHJ-S** showed the highest stability. During the catalytic cycle of **HJ** in the asymmetric Michael addition reaction, nucleophilic attack of the N atom of **HJ** on the aldehyde occurs, which eliminates H_2O to form an enamine. If H_2O molecules in the reaction system hydrolyzed the TMS group, a parasitic oxazolidine might form from the enamine, leading to the subsequent stagnation of the catalytic cycle.[38,39] In our system, immobilizing the **HJ** moiety on the polystyrene backbone (*i.e.*, **pHJ-S**) suppressed the hydrolysis of the TMS group, resulting in an improved TON. From a comparison with **pHJ-MMA**, it was suggested that choosing an appropriate polymer backbone polarity was crucial to boost both the reaction rate and the catalytic durability of water-labile organocatalysts in mechanochemical organic synthesis.

Effects of the polymer side-chain structure on catalytic performance

The catalytic performance of polymer-supported **HJ** with different side-chain structures on a polystyrene backbone (**pHJ-S**, **pHJ-^{t}BuS**, **pHJ-EGS**, **pHJ-S-^{t}BuS**, and **pHJ-S-EGS**) was further compared (Fig. 5 and Table S4). All the polymer-supported catalysts initiated the reaction while remaining as solids (Fig. S18). The polymer catalysts showed higher TONs (76 → 99, Fig. 5a, b, and Table S4) compared to **HJ** (Table 2). **pHJ-EGS** and **pHJ-S-EGS**, which had ethylene glycol moieties in their side chains, showed TOFs of 66 and 65 h^{-1}, respectively (Fig. 5b and Table S4). These TOFs were slightly higher than that of **pHJ-S** (64 h^{-1} TOF). On the other hand, **pHJ-^{t}BuS** and **pHJ-S-^{t}BuS**, which had ^{t}Bu-substituted phenyl rings, showed lower TOFs (48 and 46 h^{-1}, respectively). Through these comparative experiments, polymer-supported **HJ** with lower T_g (*i.e.*, more flexible polymer chains) showed much higher TOFs. It is noteworthy that **pHJ-S-EGS** afforded the desired product **3a** with a high enantiomeric excess (ee) of 93%, while unsupported **HJ** showed only 69% ee under mechanochemical conditions. Surprisingly, the flexible polymer catalysts accelerated the reaction in the mechanochemical Michael addition reaction.

Through comparative experiments, the thermophysical property (T_g) of the polymer-supported **HJ** was found to affect its TOF in the mechanochemical organic synthesis using a ball mill. The reaction acceleration with the flexible polymer catalyst was probably due to the following two factors: (i) a high mixing degree for solid dispersion and (ii) high contact efficiency between the reactants and catalytic sites within the polymer phase (Fig. 6).

As for (i), the ball mill provided mechanical energy to abrade and mix solid reactants in the Michael addition reaction. Subsequently, the polymer catalyst functioned as a

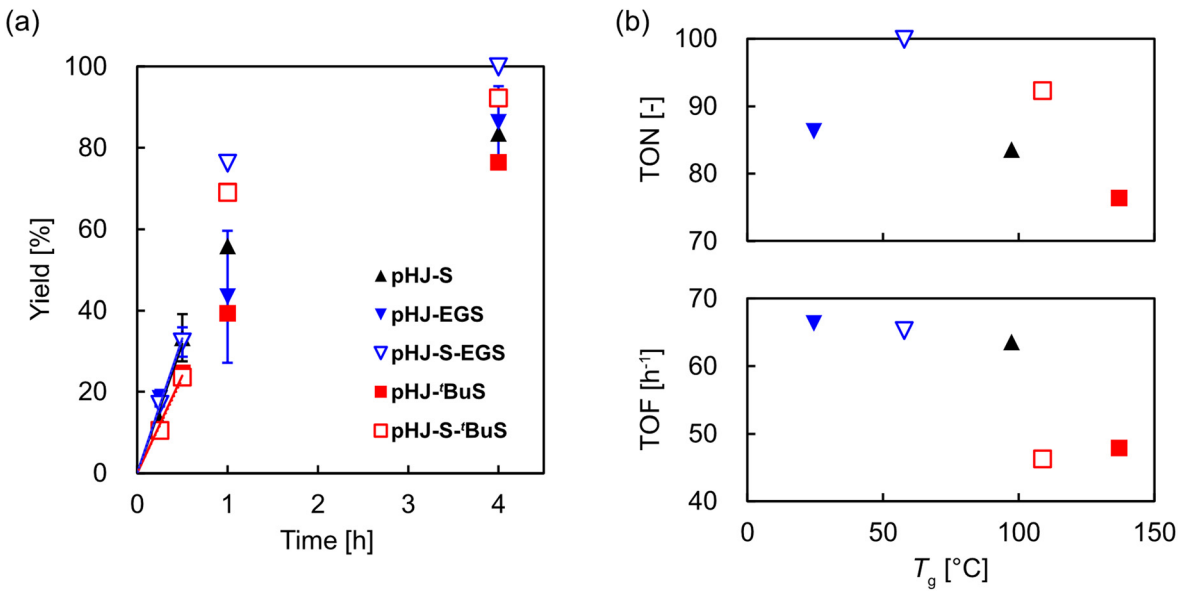

Fig. 5 (a) Time–yield profile of the Michael addition reaction using ball milling. (b) TOF and TON *vs.* T_g of polymer-supported **HJ** with different chemical structures of side chains.

 This journal is © The Royal Society of Chemistry 2026

Open Access Article. Published on 23 December 2025. Downloaded on 6/4/2026 10:27:18 PM.
This article is licensed under a Creative Commons Attribution-NonCommercial 3.0 Unported Licence.

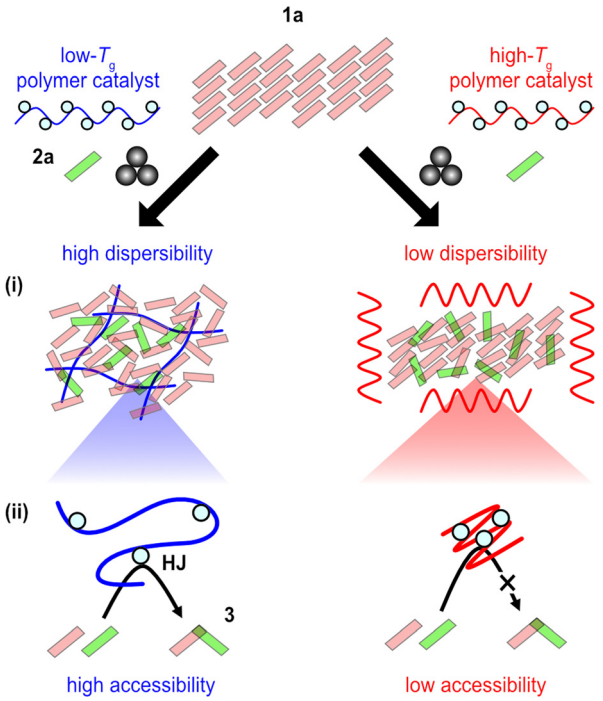

Fig. 6 Schematic of (i) a high mixing degree for solid dispersion and (ii) high contact efficiency between the reactants and catalytic sites within the polymer phase.

POLAG additive to disperse the solid reactant. Compared with rigid polymer catalysts with high T_g, the high flexibility of the polymer catalyst with low T_g could promote dispersion through mechanical deformation of the polymer chains to interact with newly generated surfaces of the solid reactants.[40]

As for (ii), the dispersed reactant should access the catalytic site within the polymer phase. It has been reported that solid-state modification of polymers with external reagents in a ball mill was pronounced within the mobile polymer phase.[41,42] These studies suggested that the flexible polymer with low T_g can smoothly accommodate external reactants in their polymer phase. Given this, the low-T_g polymer catalyst might utilize the input mechanical energy to deform its polymer chain, expose the active sites to external reactants, and facilitate reactant access for reaction acceleration. The polymer flexibility was one of the factors that determines catalytic efficiency in the solvent-less mechanochemical organic synthesis.

Substrate scope

Using the polymer-supported catalyst **pHJ-S-EGS**, we tested the substrate scope in Michael addition reactions. The reaction of **2a** with 4-bromo-(*E*)-β-nitrostyrene (**1b**) or 4-methoxy-(*E*)-β-nitrostyrene (**1c**) afforded the corresponding products (**3b** and **3c**) with high yields (80% and 75%) and stereoselectivity (80 : 20 and 85 : 15 *syn*/*anti*, Table S5). The small-molecule counterpart (**HJ**) showed low yields of **3b** and **3c** (56% and 34% respectively), which emphasized the superiority of the polymer-supported **HJ** system. When bulky aldehydes were used, the product was

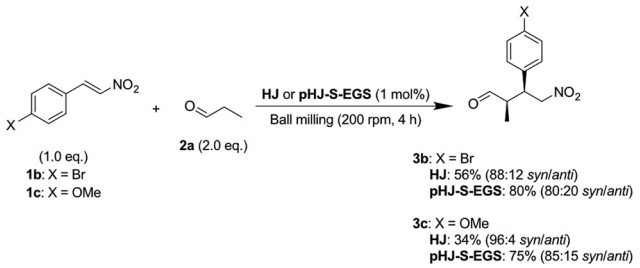

Scheme 1 Solvent-less asymmetric Michael addition reaction of substituted nitrostyrenes using ball milling. Reaction conditions: **1b** or **1c** (1.8 mmol, 1.0 eq.), **2a** (3.6 mmol, 2.0 eq.), and catalyst (1 mol% as **HJ** unit) were milled in a 20 mL ZrO_2 jar with four ZrO_2 balls (Φ = 10 mm) under an ambient atmosphere. Yields and diastereoselectivity were determined by ^{1}H NMR (xylene was used as an internal standard).

obtained in significantly lower yields (Table S5). This was likely due to inhibition of the enamine formation in the catalytic cycle of **HJ**. Throughout the screening of the scope, it was demonstrated that the excellent catalytic activity of the polymer-supported **HJ** for various nitrostyrenes (Scheme 1).

Evaluation of green metrics

Finally, the utility of polymer-supported **HJ** was further emphasized by comparison of various green metrics such as *E*-factor, PMI, and SI (Fig. 7). For all the metrics, smaller values are more desirable from a green chemistry perspective.[43] While the values for the solution system (solution (**HJ**)) exceeded 50 for all metrics, the mechanochemical systems using ball milling catalyzed by **HJ** and **pHJ-S-EGS** (**Ball milling (HJ)** and **Ball milling (pHJ-S-EGS)**) showed significantly smaller values (<2) because no solvent was used in the reaction. In the unsupported catalyst system, some of the substrates remained unreacted due to catalyst deactivation, which still needed purification of the reaction mixture to obtain pure product **3**. On

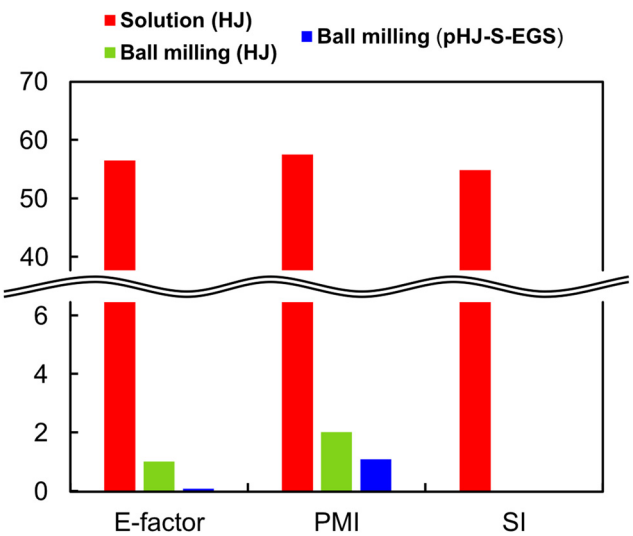

Fig. 7 Summary of green chemistry metrics. PMI = process mass intensity; SI = solvent intensity.

Open Access Article. Published on 23 December 2025. Downloaded on 6/4/2026 10:27:18 PM. This article is licensed under a Creative Commons Attribution-NonCommercial 3.0 Unported Licence.

the other hand, since almost all the substrate was converted using the polymer-supported catalyst system, all the metric values for **Ball milling (pHJ-S-EGS)** were even smaller (0.1–1.1) compared to those for **Ball milling (HJ)** (1.0–2.0), respectively. These findings in green metrics underscored the importance of solvent-less conditions and the choice of catalyst support for more efficient and greener mechanochemical synthesis.

Conclusion

In this study, the influence of the structure of polymer-supported catalysts on their catalytic activity in mechanochemical organic synthesis was investigated in the presence of solid reactants. The TOF and TON were boosted by addition of polymers as POLAG additives and the choice of an appropriate polymer backbone for the supported catalysts. Interestingly, a correlation was observed between the T_g of the polymer and the TOF. This indicates that the thermophysical properties of the polymer support governed catalytic activity in mechanochemical organic synthesis. Furthermore, the superiority of using polymer-supported catalysts was demonstrated based on green chemistry metrics. The design guidelines of polymer-supported catalysts for mechanochemical organic synthesis are expected to accelerate the development of highly efficient and more sustainable fine chemical synthesis processes under solvent-less reaction conditions.

Author contributions

KH, HM, and YM designed the experiments. KH performed the experiments. HK and EN supported the *in situ* PXRD measurements. KH, HM, and YM wrote the manuscript. MN, HK, and EN contributed to discussions during this work. All authors have read and approved the final version of the manuscript.

Conflicts of interest

There are no conflicts to declare.

Data availability

The authors confirm that the data supporting the findings of this study are available within the article and its supplementary information (SI). Supplementary information: materials and methods, synthetic procedures, EDX and thermographic analyses, and NMR spectra. See DOI: https://doi.org/10.1039/d5gc05291b.

Acknowledgements

We greatly appreciate Prof. Dr Inoue at Kyushu University for providing the planetary mill and supporting the experiments with the ball mill. This work was supported by JSPS KAKENHI grant numbers JP24K17560, JP23K26708, the Environment Research and Technology Development Fund (JPMEERF20255RB4) of the Environmental Restoration and Conservation Agency (ERCA) provided by the Ministry of the Environment of Japan, the Sumitomo Foundation, the Yashima Environment Technology Foundation, and the Tobemaki Foundation. This article is based on results obtained from a project, JPNP20004, subsidized by the New Energy and Industrial Technology Development Organization (NEDO). The synchrotron experiments were performed at SPring-8 BL13XU with the approval of the Japan Synchrotron Radiation Research Institute (JASRI) (Proposal No. 2024B1782 and 2024B1977).

References

1 P. Anastas, M. Nolasco, F. Kerton, M. Kirchhof, P. Licence, T. Pradeep, B. Subramaniam and A. Moores, *ACS Sustainable Chem. Eng.*, 2021, **9**, 8015–8017.
2 D. J. C. Constable, C. Jimenez-Gonzalez and R. K. Henderson, *Org. Proc. Res. Dev.*, 2007, **11**, 133–137.
3 C. Jimenez-Gonzalez, C. S. Ponder, Q. B. Broxterman and J. B. Manley, *Org. Proc. Res. Dev.*, 2011, **15**, 912–917.
4 R. A. Sheldon, *Green Chem.*, 2017, **19**, 18–43.
5 G. W. Wang, *Chem. Soc. Rev.*, 2013, **42**, 7668.
6 T. K. Achar, A. Bose and P. Mal, *Beilstein J. Org. Chem.*, 2017, **13**, 1907–1931.
7 V. Némethová, D. Krištofíková, M. Mečiarová and R. Šebesta, *Chem. Rec.*, 2023, **23**, e202200283.
8 K. Kubota, *Bull. Chem. Soc. Jpn.*, 2023, **96**, 913–930.
9 D. Braga, L. Maini and F. Grepioni, *Chem. Soc. Rev.*, 2013, **42**, 7638–7648.
10 Y. Xiao, C. Wu, X. Hu, K. Chen, L. Qi, P. Cui, L. Zhou and Q. Yin, *Cryst. Growth Des.*, 2023, **23**, 4680–4700.
11 A. Krusenbaum, S. Grätz, G. T. Tigineh, L. Borchardt and J. G. Kim, *Chem. Soc. Rev.*, 2022, **51**, 2873–2905.
12 J. Li, C. Nagamani and J. S. Moore, *Acc. Chem. Res.*, 2015, **48**, 2181–2190.
13 A. Taghipour, A. Rahimpour, M. Rastgar and M. Sadrzadeh, *Ultrason. Sonochem.*, 2022, **90**, 106202.
14 J. Andersen and J. J. Mack, *Green Chem.*, 2018, **20**, 1435.
15 Q. T. Trinh, N. Golio, Y. Cheng, H. Ha, K. U. Tai, L. Ouyang, J. Zhao, T. S. Tran, T. K. Nguyen, J. Zhang, H. An, Z. Wei, F. Jerome, P. N. Amaniamapong and N. T. Nguyen, *Green Chem.*, 2025, **27**, 4926.
16 A. Stolle, T. Szuppa, S. E. S. Leonhardt and B. Ondruschka, *Chem. Soc. Rev.*, 2011, **40**, 2317–2329.
17 J. G. Hernández and C. Bolm, *J. Org. Chem.*, 2017, **82**, 4007–4019.
18 Z. J. Jiang, Z. H. Li, J. B. Yu and W. K. Su, *J. Org. Chem.*, 2016, **81**, 10072–10078.
19 K. Kubota, T. Seo, K. Koide, Y. Hasegawa and H. Ito, *Nat. Commun.*, 2019, **10**, 111.

 This journal is © The Royal Society of Chemistry 2026

Open Access Article. Published on 23 December 2025. Downloaded on 6/4/2026 10:27:18 PM.
This article is licensed under a Creative Commons Attribution-NonCommercial 3.0 Unported Licence.

20 P. Ying, T. Ying, H. Chen, K. Xiang, W. Su, H. Xie and J. Yu, *Org. Chem. Front.*, 2024, **11**, 127–134.
21 A. M. Belenguer, G. I. Lampronti, A. J. Cruz-Cabeza, C. A. Hunter and J. K. M. Sanders, *Chem. Sci.*, 2016, **7**, 6617–6627.
22 A. Mascitti, M. Lupacchini, R. Guerra, I. Taydakov, L. Tonucci, N. d'Alessandro, F. Lamaty, J. Martinez and E. Colacino, *Beilstein J. Org. Chem.*, 2017, **13**, 19–25.
23 L. Konnert, M. Dimassi, L. Gonnet, L. Lamaty, F. Martinez and E. Colacino, *RSC Adv.*, 2016, **6**, 36978.
24 V. Declerck, E. Colacino, X. Bantreil, J. Martinez and F. Lamaty, *Chem. Commun.*, 2012, **48**, 11778–11780.
25 K. Kubota, T. Seo and H. Ito, *Faraday Discuss.*, 2023, **241**, 104.
26 T. Seo, K. Kubota and H. Ito, *J. Am. Chem. Soc.*, 2023, **145**, 6823–6837.
27 K. Xiang, H. Shou, C. Hu, W. Su and J. Yu, *Green Chem.*, 2024, **26**, 5890.
28 Y. Hayashi, H. Gotoh, T. Hayashi and M. Shoji, *Angew. Chem., Int. Ed.*, 2005, **44**, 4212–4215.
29 K. A. Jørgensen, M. Johannsen, S. Yao, H. Audrain and J. Thorhauge, *Acc. Chem. Res.*, 1999, **32**, 605–613.
30 M. Pagliaro, V. Pandarus, R. Ciriminna, F. Bland and P. D. Carà, *ChemCatChem*, 2012, **4**, 1013–1018.
31 Y. Hayashi, S. Hattori and S. Koshino, *Chem. – Asian J.*, 2022, **17**, e202200314.
32 H. Ochiai, A. Nishiyama, N. Haraguchi and S. Itsuno, *Org. Process Res. Dev.*, 2020, **24**(10), 2228–2233.
33 H. Shigeeda, H. Matsumoto, M. Nagao and Y. Miura, *React. Chem. Eng.*, 2025, **10**, 1038–1046.
34 Y. Zheng, H. Kasai, S. Kobayashi, S. Kawaguchi and E. Nishibori, *Mater. Adv.*, 2023, **4**, 1005–1010.
35 Y. Yano, H. Kasai, Y. Zheng, E. Nishibori, Y. Hisada and T. Ono, *Angew. Chem., Int. Ed.*, 2022, **61**, e202203853.
36 J. Haraada, M. Harakawa and K. Ogawa, *CrystEngComm*, 2009, **11**, 638–642.
37 L. Zahir, N. J. Ara and S. I. Chowdhury, *Chem. Sci. Eng. Res.*, 2020, **2**, 34–38.
38 M. B. Schmid, K. Zeiter and R. M. Gschwind, *J. Am. Chem. Soc.*, 2011, **133**, 7065–7074.
39 O. V. Maltsev, O. A. Chizhov and S. G. Zlotin, *Chem. – Eur. J.*, 2011, **17**, 6109–6117.
40 C. Asgreen, M. M. Knopp, J. Skytte and K. Löbmann, *Pharmaceutics*, 2020, **12**, 483.
41 C. Gerbehaye, K. V. Bernaerts, R. Mincheva and J. M. Raquez, *Eur. Polym. J.*, 2022, **166**, 111010.
42 J. J. P. Bravo, C. Gerbehaye, J. M. Raquez and R. Mincheva, *Molecules*, 2024, **29**, 667.
43 N. Fantozzi, J. N. Volle, A. Porcheddu, D. Virieux, F. García and E. Colacino, *Chem. Soc. Rev.*, 2023, **52**, 6680–6714.